Topological superconductivity enhanced by exceptional points

R. Arouca ⊙,* Jorge Cayao,† and Annica M. Black-Schaffer ⊙‡

Department of Physics and Astronomy, Uppsala University, Uppsala SE-75120, Sweden

Majorana zero modes (MZMs) emerge as edge states in topological superconductors and are promising for topological quantum computation, but their detection has so far been elusive. Here we show that non-Hermiticity can be used to obtain dramatically more robust MZMs. The enhanced properties appear as a result of an extreme instability of exceptional points to superconductivity, such that even a vanishingly small superconducting order parameter already opens a large energy gap, produces well-localized MZMs, and leads to strong superconducting pair correlations. Our work thus illustrates the large potential of enhancing electronic ordering, here in the form of topological superconductivity, using non-Hermitian exceptional points.

Introduction. Topological superconductors are currently intensively pursued since they can host Majorana zero modes (MZMs), which are promising for topological quantum computation due to their non-Abelian statistics [1,2]. The simplest model to present topological superconductivity is the Kitaev chain [3–33]. While being a simple model composed of spinless fermions with p-wave pairing, it is still effectively realized at interfaces between conventional superconductors and topological insulators [34–39], semiconductors [40–46], and even using magnetic impurity chains [47–56].

In the ideal situation, MZMs emerge at zero energy and are well separated from the quasicontinuum of other states by a topological gap, which creates an isolated subspace for the topological qubit. However, in practice, the topological gap strongly depends on material properties and is usually smaller than the superconducting order parameter in the parent superconductor. This considerably limits a realistic Majorana-based computation [2,57], which urgently calls for platforms with much larger values of the topological gap.

With the advent of non-Hermitian quantum mechanics, it has been predicted that system properties can be drastically enhanced due to the strong sensitivity of non-Hermitian systems [58–62]. This sensitivity is due to the presence of non-Hermitian degeneracies, also known as exceptional points (EPs), which are points where both eigenvalues and eigenstates coalesce [59,63–90]. The sensitivity gets even larger when increasing the number N of coalescing energy levels, where N is also referred to as the order of the EP. In fact, for a dimensionless perturbation x, the spectrum changes as $x^{1/N}$ [58–62], revealing that even an infinitesimally small x can induce a sizable effect for sufficiently large N. A tantalizing question arises here if it may be possible to exploit this strong sensitivity of non-Hermitian systems to enhance the topological gap protecting the MZMs.

In this work, we show that non-Hermiticity can dramatically enhance topological superconductivity, producing much more robust MZMs. In particular, we consider the nonreciprocal Kitaev chain and show that the presence of a high-order EP in the normal state makes the system highly unstable to superconductivity, such that even a vanishingly small superconducting order parameter is sufficient to open a sizable gap protecting the MZMs, resulting in exceptionally enhanced topological superconductivity. With sizable superconductivity being hard to achieve experimentally, our results open a compelling avenue for designing systems with much more robust MZMs.

Model and its normal state. To investigate and most clearly elucidate exceptionally enhanced topological superconductivity, we consider a non-Hermitian extension of the simplest known topological superconductor: the Kitaev chain. Further, as we want to investigate systems with strong non-Hermitian sensitivity, we seek a very simple model where the normal state presents a high-order EP. An ideal candidate for the latter is the Hatano-Nelson (HN) model [81,91,92], where simple nonreciprocal hoppings give rise to high-order EP [81,91,92]. Combining the two models we arrive at the Hatano-Nelson-Kitaev (HNK) chain, which is illustrated in Fig. 1 and given by

$$H = -\sum_r \left[(t + \Gamma)c_{r+1}^\dagger c_r + (t - \Gamma)c_r^\dagger c_{r+1} + \mu c_r^\dagger c_r \right]$$
$$+ \sum_r (\Delta c_{r+1}^\dagger c_r^\dagger + \text{H.c.}), \tag{1}$$

where $c_r^\dagger$ (c_r) creates (annihilates) a spinless fermion at site r, t is the nearest-neighbor hopping, μ the chemical potential, Δ the p-wave superconducting order parameter, and Γ encodes the nonreciprocity.

*rodrigo.arouca@physics.uu.se
†jorge.cayao@physics.uu.se
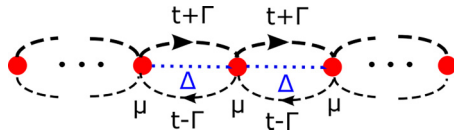‡annica.black-schaffer@physics.uu.se

FIG. 1. Lattice representation of the HNK Hamiltonian with lattice sites (red dots) and terms connecting different sites (dashed/dotted lines).

The Hermitian, or Kitaev, limit, found at $\Gamma = 0$, hosts a topological phase for $|\mu/t| < 2$, characterized by a bulk topological invariant and MZMs at the endpoints of any finite chain [3–6]. Inclusion of the nonreciprocal Γ into the Kitaev chain has already been considered [28–30]. Even though non-Hermitian systems can present new topological phases or extend the topological phases in Hermitian systems [81,93], the topological phase diagram for the HNK chain was found to remain, being characterized by the non-Hermitian version of the same invariant [28] and showing localized MZMs. It has additionally been shown that the non-Abelian braiding is preserved in non-Hermitian systems [69,94]. These earlier results seem to indicate that one does not gain much from making the Kitaev chain non-Hermitian. However, an entirely overlooked aspect is how the normal-state EPs can dramatically enhance the topological superconducting phase, albeit the phase diagram boundaries do not change.

Before showing that the EP in the normal-state spectrum enhances the superconducting phase, we need to describe this EP. The normal state of the HNK chain in just the HN model [81,91,92] or Eq. (1) with $\Delta = 0$. Due to the nonreciprocal hopping, the HN model presents remarkably different properties depending on the boundary conditions. In the presence of periodic boundary conditions (PBC), it hosts non-Hermitian topological phases but no EPs. In contrast, the open boundary conditions (OBC) system does not have a topological phase but has an EP of the order of the system size L [81,91,92]. As we are interested in the EP effects and MZMs, we focus on OBC in the main text but discuss the PBC system in the Supplemental Material (SM) [95] (see also Refs. [96–101] therein). In general, for non-Hermitian systems, the bulk spectrum for OBC can be captured by the non-Bloch Hamiltonian h, which takes values in a complex generalization of the Brillouin zone [102–104]. In many cases, including the HN model, we can then obtain an analytical expression for the eigenvalues of h and, consequently, of the OBC spectrum [102–104]. However, for the HNK chain, to the best of our knowledge, there exists no analytical solution, see SM [95]. Therefore, we are here forced to primarily rely on a numerical solution of the Boguliubov-de Gennes (BdG) Hamiltonian [105,106], where $H = \mathbb{C}^\dagger \mathbb{H}_{\text{BdG}} \mathbb{C}$, using the Nambu vector $\mathbb{C} = (c_0 \ \cdots \ c_{L-1} \ c_0^\dagger \ \cdots \ c_{L-1}^\dagger)^T$, for an open chain with L sites. The real/imaginary parts of the spectrum of Eq. (1) in the normal state are shown in Figs. 2(a), 2(c) as a function of Γ/t. For $|\Gamma/t| < 1$, the energies are completely real, while for $|\Gamma/t| > 1$, the energies are purely imaginary. The presence of regions with completely real energies in the system is due to pseudo-Hermitian ($\mathcal{PH}$) symmetry, while the developing of a spectrum with complex conjugated pairs marks the spontaneous breaking of this symmetry [107–111].
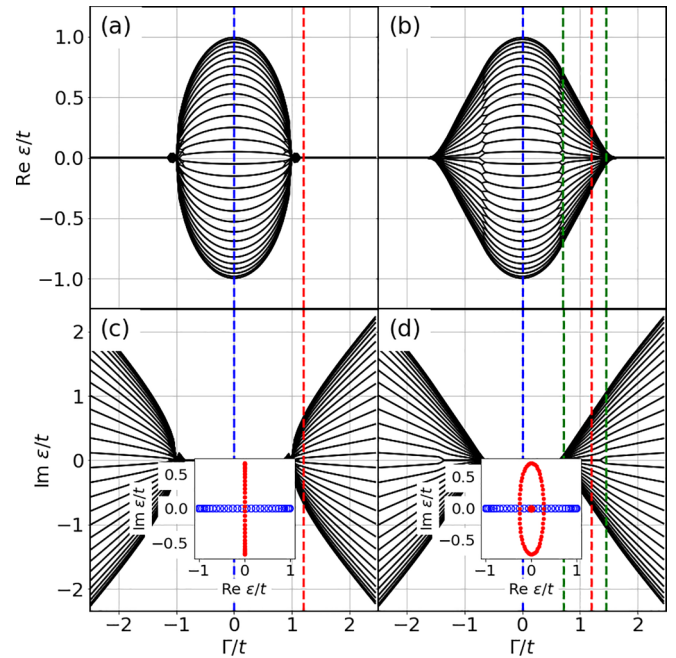

FIG. 2. Spectrum of the OBC HNK system as a function of Γ/t with (a), (c) $\Delta = 0$ and (b), (d) $\Delta = 10^{-10}t$. First (second) row shows the real (imaginary) part of the energy spectrum. Insets in (c), (d) show the energy levels in the complex plane in the Hermitian limit ($\Gamma = 0$, blue dashed lines and open circles) and in the $\mathcal{PH}$-broken phase ($\Gamma = 1.2t$, red dashed lines and filled circles). Green dashed lines mark the region with MZMs. Other parameters: $\mu = 0, L = 30$.

These $\mathcal{PH}$-preserved and $\mathcal{PH}$-broken phases are separated by an EP of the order of the system size, where all energy levels coalesce [81,91,92].[1]

Exceptional gap. Having understood the HNK system without superconductivity and its EP, we next add a small superconducting order parameter Δ. Doing so, we arrive at a surprising conclusion: already adding a vanishingly small Δ dramatically changes the energy levels. In Figs. 2(b), 2(d) we show the real/imaginary part of the spectrum for the extremely small $\Delta = 10^{-10}t$ (see SM [95] for complementary data at different L). For such small values of Δ, most of the spectrum barely changes from the nonsuperconducting case. The exception is for Γ values around the normal-state EP, which disappears and is replaced by a continuum of bands, which joins pairwise in multiple EPs. In addition, there are also two zero-energy states, two MZMs, clearly isolated from the rest of the other modes, easily seen when plotting the complex energies (red filled circles) in the inset of Fig. 2(d). We further notice that although these MZMs are clearly isolated modes, there still exist bulk modes with, separately, $\text{Re}(\epsilon) = 0$ or $\text{Im}(\epsilon) = 0$. Thus, one may naively think the system is gapless, just as in the Hermitian limit (blue circles), but thanks to the

—————

[1] In the non-Bloch formalism, this complete coalescence can be understood as a non-Bloch band collapse [104,107–110], where the imaginary part of the momentum diverges for all modes, such that the energies accumulate at a single value, see, e.g., Ref. [137] for a discussion in the HN model.
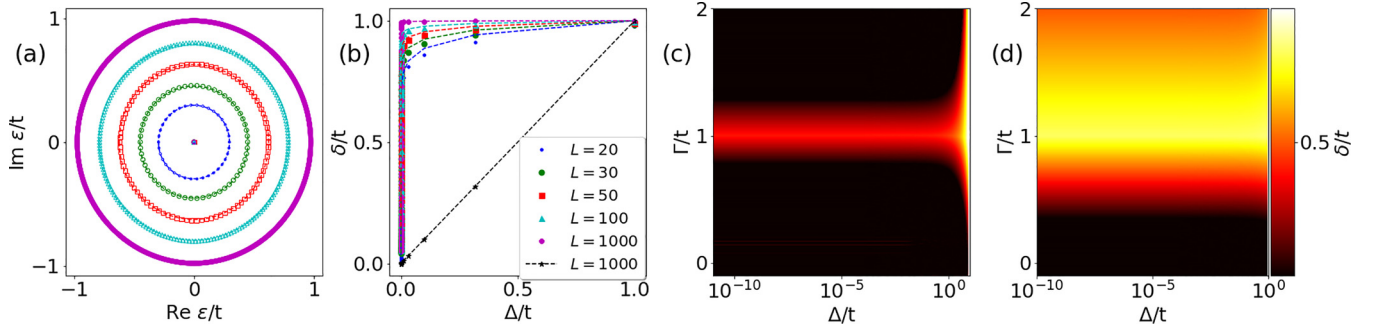
FIG. 3. Exceptional sensitivity of (a) the spectrum ϵ and (b) minigap δ for $\Gamma = t$ or $\Gamma = 0$ at multiple different systems sizes L, using $\Delta = 10^{-10}t$. Points represent numerical data, the dashed lines analytical results [Eq. (2)]. Minigap δ as a function of Δ/t and Γ/t for (c) $L = 30$ and (d) $L = 100$. Other parameters: $\mu = 0$.

complex energy spectrum, there exists a finite region in the complex plane around the MZMs where no bulk states are found. This spectrum configuration corresponds to a point gap, which provides a non-Hermitian topological protection of the MZMs [81]. As a consequence, even for a vanishingly small Δ, we find a finite minigap $\delta = |\epsilon_{QP} - \epsilon_{MZM}|$, with ϵ_{QP} being the lowest quasiparticle mode, protecting the MZMs. The finite minigap exists for a finite range of Γ, marked by the vertical green dashed lines in Figs. 2(b), 2(d). Although we find no general analytical expression for the minigap protecting the MZM, we can gain understanding by perturbatively adding superconducting pairing at the normal-state EP. The details are given in the SM [95] and here we focus on the results. At $\Gamma/t = 1$, the (bulk) energy levels ϵ_m are given, to the lowest order in Δ/t, by

$$\epsilon_m/t \approx \exp\left(i\pi m \frac{L}{2L-2}\right)^{L-1}\sqrt{\Delta/t}, \qquad (2)$$

with $m = 0, 1, \ldots, 2L - 2$. From this result, we see that for sufficiently large L, $^{L-1}\sqrt{\Delta/t} \sim 1$ for any Δ, which directly explains the exceptional sensitivity of the energy levels to any perturbation Δ. This result is in agreement with the recently reported sensitivity of non-Hermitian systems [66,112], but they were not considering superconductivity or other electronic ordering. This approximate energy level expression also clarifies why the energies are complex since each of them is a point on a circle in the complex plane. The radius of this circle also automatically gives the minigap, $\delta/t \approx (\Delta/t)^{1/(L-1)}$ since the MZMs are at zero energy. In Figs. 3(a), 3(b), we compare the approximate analytical results for the energy levels [Fig. 3(a)] and minigap [Fig. 3(b)] with the earlier obtained exact numerical results using $\Gamma/t = 1$ and $\Delta/t = 10^{-10}$ for many different values of L. We find that analytical (lines) and numerical (points) results agree so well with each other that they are not distinguishable in the figure. We also directly see that as L increases, the radii of the energy level circles increase, leaving a larger minigap. In particular, we notice that the $(L - 1)$-root expression in Eq. (2) means that there is a power-law behavior of the minigap δ, as we show in the SM [95]. This is very different from the Hermitian limit (black points, lines) where the minigap is always $\delta \sim \Delta$. We thus establish, both numerically and analytically, that the normal-state EP makes the system exceptionally unstable in the thermodynamic limit to superconductivity,

generating a finite minigap even for vanishingly small Δ. It is the coalescence of all levels at the normal-state EP that generates this extreme instability as a collective phenomenon.

The above analytical analysis is only valid at the normal-state EP at $\Gamma/t = 1$, but the instability towards superconductivity extends for a finite range of Γ around the EP. We illustrate this in Figs. 3(c), 3(d) where we plot the minigap δ as a function of both Γ and Δ for both $L = 30$ [Fig. 3(c)] and $L = 100$ [Fig. 3(d)]. The strong system-size dependence is also visible here, as a sizable minigap is present in a much larger region for the larger L system, clearly emphasizing the collective aspect of the effect. The spectrum is also affected by other values of the parameters, but MZMs are still present in a large region of the parameter space. For instance, although we here only report data for $\mu = 0$, for $\Delta = 10^{-10}t$ the enhancement appears in the large regime $|\mu/t| \lesssim 1$. To not deviate from the main result, we discuss these details in the SM and in supplemental videos (SVs) [95].

Taken together, we find that already a vanishingly small Δ around the normal-state EP changes the features of the spectrum in the complex plane, opening a sizable point gap that produces isolated MZMs. We coin this remarkable sensitivity exceptionally enhanced topological superconductivity. The sensitivity is a collective effect, arising due to the accumulation of all system modes at the EP and thus growing with system size. This can be viewed as a non-Hermitian equivalent of how the accumulation of density of states in flat band systems creates superconductivity, as well as other electronic ordered states, as recently illustrated in, e.g., twisted bilayer graphene at the magic angle [113–116] or bi- and trilayer graphene in electric fields [117,118].

Robust MZMs and superconductivity. Exceptional topological superconductivity is not restricted to influencing the topological gap, but next we show how it also manifests in the spectral weight and superconducting pair correlations. These are encoded in the Nambu Green's function $\mathcal{G}$ [87,100,119,120][2]

$$\mathcal{G}(\omega) = \frac{1}{\hbar\omega\hat{1} - \mathbb{H}_{BdG}} = \begin{pmatrix} G_e & F_{eh} \\ F_{he} & G_h \end{pmatrix}, \qquad (3)$$

---

[2]We include a small $(10^{-7}t)$ imaginary positive term in $\hbar\omega$ in the definition of $\mathcal{G}$ to obtain finite line widths for modes with zero imaginary part.
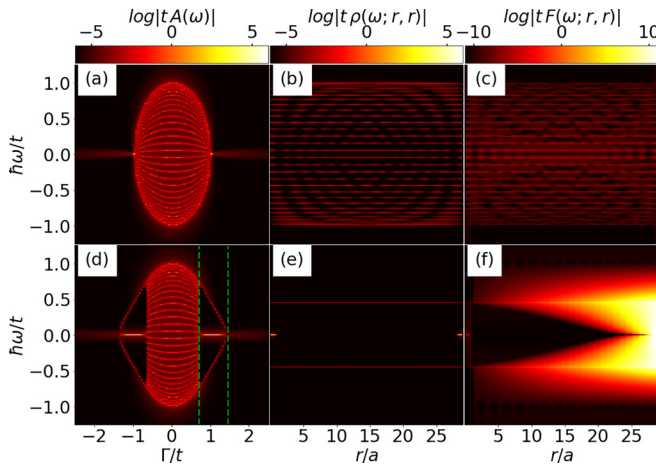
FIG. 4. (a), (d) Spectral weight A, (b), (c) LDOS ρ, and local superconducting pair correlations (c), (f) F as a function of Γ, ω and position r along the chain (a is the lattice parameter). First column shows A for $\Delta = 0$ (a) and $\Delta = 10^{-10}t$ (d), second column shows ρ for $\Delta = 10^{-10}t$ and $\Gamma = 0$ (b) and $\Gamma = t$ (e), and the third column shows F for $\Delta = 10^{-10}t$ and $\Gamma = 0$ (c) and $\Gamma = t$ (f). Other parameters: $L = 30$, $\mu = 0$.

where G_e and G_h are the normal electron and hole Green's functions, respectively, while F_{eh} and F_{he} are the anomalous contributions containing the superconducting pair correlations or amplitudes. From $\mathcal{G}$, we obtain all two-particle observables of the system, see SM [95] for details. First, we calculate the spectral weight $A(\omega) = -\text{Im Tr}[\mathcal{G}(\omega) - \mathcal{G}^{\dagger}(\omega)]/(2\pi)$, which represents the density of states at the frequency (energy) ω ($\hbar\omega$). Note that Tr here denotes the sum over both electron and hole components and spatial coordinates. In Figs. 4(a), 4(d) we plot A for the HNK system. At $\Delta = 0$ [Fig. 4(a)], A is only finite when $\mathcal{PH}$ symmetry is preserved, and we find mainly nonzero real energy values. The only visible peak occurs at the normal-state EP ($|\Gamma/t| = 1$) due to its accumulation of modes. For a vanishingly small $\Delta = 10^{-10}t$ [Fig. 4(d)], the same behavior, with A reflecting the nonzero real part of the spectrum, is now only found in a narrower region of Γ. Instead, there is a huge peak at $\omega = 0$ that extends until the real energies disappear. This is the same region, marked by green dashed lines in Fig. 2, where we find a point gap separating the MZMs from the remaining modes. Thus, this peak in A is nothing other than a zero-bias peak (ZBP) produced by the MZMs [5,6]. Moreover, since the sizable point gap is associated with finite imaginary energies, which broadens the poles for all modes but the MZMs, we find a very clear ZBP with no other low-energy spectral weight, again signaling the exceptional enhancement of the topological phase.

The exceptional enhancement is not only seen in the spectrum and spectral weight but also in the spatial properties of the system. To illustrate this, we consider the local density of states (LDOS), $\rho(\omega; r) = -\text{Im}[G_e(\omega; r, r)]/\pi$. In Fig. 4(b), we plot ρ as a function of position along the chain for $\Delta = 10^{-10}t$ in the Hermitian limit ($\Gamma = 0$) and find, as expected, essentially uniform occupation across energies and position. In contrast, tuning to the normal-state EP at $\Gamma = t$ in Fig. 4(c), we find very pronounced and well-localized peaks at zero energy at each end of the chain. This demonstrates that

non-Hermiticity also strongly promotes MZM localization, which, together with the large minigap, establishes the existence of robust MZMs. Farther away from the EP, we still find MZMs, but they then decay further into the bulk, see SV [95], since the coherence length of the MZMs is proportional to δ^{-1} [5,6].

Finally, we also show that the superconducting pair correlations, expressed through F_{eh}, are also exceptionally enhanced due to the normal-state EP. Keeping a vanishingly small $\Delta = 10^{-10}t$, we find in the Hermitian limit in Fig. 4(c) that the local pair correlations are of the same order as Δ and delocalized in the lattice, as expected. In contrast, for $\Gamma = t$ in Fig. 4(f), we find an excessively strong F, up to 20 orders of magnitude larger than Δ. Such a strong response shows that, although the superconducting order parameter Δ is vanishingly small, there exists strong superconducting pairing, further cementing the notion of exceptionally enhanced topological superconductivity. Another remarkable feature is the localization of F_{eh} at the right edge due to the non-Hermitian skin effect [73,102–104,121–132]. If instead plotting F_{he}, we find a similar localization at the left edge, illustrating that electron and hole components localize on opposite edges.

Concluding remarks. We show that even a vanishingly small superconducting order parameter Δ in a nonreciprocal Kitaev chain can create exceptional topological superconductivity with robust MZMs, due to a normal-state EP of the order of the system size. The robustness of the MZMs stems from the opening of an exceptionally enhanced point gap in the system, which both generates the minigap protecting the MZMs and strongly localized MZMs. Moreover, the superconducting pair correlations are also exceptionally enhanced. While the most dramatic behavior occurs for vanishingly small Δ close to the normal-state EP, any non-Hermiticity still enhances MZM robustness and superconductivity. Our results are also stable to changes in the chemical potential. We expect that this relative insensitivity to parameter values also makes the results stable to weak disorder. In terms of a direct experimental realization, cold atom systems are promising as they can host both p-wave pairing [36,133] and nonreciprocity [79,92]. Our results are also transferable to other superconductors as they only require the opening of a point gap close to an EP in the normal state. Additionally, we speculate that the same reasoning can be applied to other correlated phases that are amplified by state degeneracies, simple examples being the Stoner mechanism for ferromagnetism [134] and the Peierls instability [135]. Finally, an interesting outlook is to understand the role of particle-hole symmetry in exceptionally enhanced superconductivity, since the enhancement of the gap with a power $1/(L - 1)$, while preserving MZMs, seems to be related to the analysis of perturbations of EPs in the presence of chiral and sublattice symmetry in Ref. [136].

[1] C. Beenakker, SciPost Phys. Lect. Notes 15 (2020).

[2] S. D. Sarma, M. Freedman, and C. Nayak, npj Quantum Inf. **1**, 15001 (2015).

[3] A. Y. Kitaev, Phys.-Usp. **44**, 131 (2001).

[4] C. Beenakker, Annu. Rev. Condens. Matter Phys. **4**, 113 (2013).

[5] R. Aguado, Riv. Nuovo Cimento **40**, 523 (2017).

[6] K. Flensberg, F. von Oppen, and A. Stern, Nat. Rev. Mater. **6**, 944 (2021).

[7] Y. Tanaka, M. Sato, and N. Nagaosa, J. Phys. Soc. Jpn. **81**, 011013 (2012).

[8] Y. Tanaka and S. Kashiwaya, Phys. Rev. B **56**, 892 (1997).

[9] Y. Tanaka and S. Kashiwaya, Phys. Rev. B **53**, R11957 (1996).

[10] S. Nakosai, J. C. Budich, Y. Tanaka, B. Trauzettel, and N. Nagaosa, Phys. Rev. Lett. **110**, 117002 (2013).

[11] D. Pikulin and Y. V. Nazarov, JETP Lett. **94**, 693 (2012).

[12] X. Wang, T. Liu, Y. Xiong, and P. Tong, Phys. Rev. A **92**, 012116 (2015).

[13] C. Yuce, Phys. Rev. A **93**, 062130 (2016).

[14] Q.-B. Zeng, B. Zhu, S. Chen, L. You, and R. Lü, Phys. Rev. A **94**, 022119 (2016).

[15] M. Klett, H. Cartarius, D. Dast, J. Main, and G. Wunner, Phys. Rev. A **95**, 053626 (2017).

[16] C. Li, X. Z. Zhang, G. Zhang, and Z. Song, Phys. Rev. B **97**, 115436 (2018).

[17] K. Kawabata, Y. Ashida, H. Katsura, and M. Ueda, Phys. Rev. B **98**, 085116 (2018).

[18] A. McDonald, T. Pereg-Barnea, and A. A. Clerk, Phys. Rev. X **8**, 041031 (2018).

[19] J. Avila, F. Peñaranda, E. Prada, P. San-Jose, and R. Aguado, Commun. Phys. **2**, 133 (2019).

[20] S. Lieu, Phys. Rev. B **100**, 085110 (2019).

[21] J. Cayao, C. Triola, and A. M. Black-Schaffer, Eur. Phys. J. Spec. Top. **229**, 545 (2020).

[22] C. Li, L. Jin, and Z. Song, Sci. Rep. **10**, 6807 (2020).

[23] A. Maiellaro and R. Citro, J. Phys.: Conf. Ser. **1548**, 012026 (2020).

[24] L. Zhou, Phys. Rev. B **101**, 014306 (2020).

[25] Z.-H. Wang, F. Xu, L. Li, D.-H. Xu, and B. Wang, Phys. Rev. B **104**, 174501 (2021).

[26] X.-P. Jiang, Y. Qiao, and J. Cao, Chin. Phys. B **30**, 077101 (2021).

[27] T. Liu, S. Cheng, H. Guo, and G. Xianlong, Phys. Rev. B **103**, 104203 (2021).

[28] Y. Li, Y. Cao, Y. Chen, and X. Yang, J. Phys.: Condens. Matter **35**, 055401 (2023).

[29] S. Rahul and S. Sarkar, Sci. Rep. **12**, 6993 (2022).

[30] X.-M. Zhao, C.-X. Guo, S.-P. Kou, L. Zhuang, and W.-M. Liu, Phys. Rev. B **104**, 205131 (2021).

[31] Z.-H. Wang, F. Xu, L. Li, D.-H. Xu, W.-Q. Chen, and B. Wang, Phys. Rev. B **103**, 134507 (2021).

[32] C. Zhang, L. Sheng, and D. Xing, Phys. Rev. B **103**, 224207 (2021).

[33] D. I. Pikulin and Y. V. Nazarov, Phys. Rev. B **87**, 235421 (2013).

[34] L. Fu and C. L. Kane, Phys. Rev. B **79**, 161408(R) (2009).

[35] Y. Tanaka, T. Yokoyama, and N. Nagaosa, Phys. Rev. Lett. **103**, 107002 (2009).

[36] A. Bühler, N. Lang, C. V. Kraus, G. Möller, S. D. Huber, and H. P. Büchler, Nat. Commun. **5**, 4504 (2014).

[37] A. M. Black-Schaffer and A. V. Balatsky, Phys. Rev. B **87**, 220506(R) (2013).

[38] A. Banerjee, A. Sundaresh, R. Ganesan, and P. A. Kumar, ACS Nano **12**, 12665 (2018).

[39] D. Culcer, A. C. Keser, Y. Li, and G. Tkachov, 2D Mater. **7**, 022007 (2020).

[40] R. M. Lutchyn, J. D. Sau, and S. Das Sarma, Phys. Rev. Lett. **105**, 077001 (2010).

[41] Y. Oreg, G. Refael, and F. von Oppen, Phys. Rev. Lett. **105**, 177002 (2010).

[42] V. Mourik, K. Zuo, S. M. Frolov, S. Plissard, E. P. Bakkers, and L. P. Kouwenhoven, Science **336**, 1003 (2012).

[43] S. Nakosai, Y. Tanaka, and N. Nagaosa, Phys. Rev. Lett. **108**, 147003 (2012).

[44] J. Cayao, P. San-Jose, A. M. Black-Schaffer, R. Aguado, and E. Prada, Phys. Rev. B **96**, 205425 (2017).

[45] J. Cayao, A. M. Black-Schaffer, E. Prada, and R. Aguado, Beilstein J. Nanotechnol. **9**, 1339 (2018).

[46] J. Cayao and A. M. Black-Schaffer, Eur. Phys. J. Spec. Top. **227**, 1387 (2018).

[47] T.-P. Choy, J. M. Edge, A. R. Akhmerov, and C. W. J. Beenakker, Phys. Rev. B **84**, 195442 (2011).

[48] S. Nadj-Perge, I. K. Drozdov, B. A. Bernevig, and A. Yazdani, Phys. Rev. B **88**, 020407(R) (2013).

[49] F. Pientka, L. I. Glazman, and F. von Oppen, Phys. Rev. B **88**, 155420 (2013).

[50] S. Nadj-Perge, I. K. Drozdov, J. Li, H. Chen, S. Jeon, J. Seo, A. H. MacDonald, B. A. Bernevig, and A. Yazdani, Science **346**, 602 (2014).

[51] S. Nakosai, Y. Tanaka, and N. Nagaosa, Phys. Rev. B **88**, 180503(R) (2013).

[52] K. Björnson and A. M. Black-Schaffer, Phys. Rev. B **94**, 100501(R) (2016).

[53] M. Mashkoori, S. Pradhan, K. Björnson, J. Fransson, and A. M. Black-Schaffer, Phys. Rev. B **102**, 104501 (2020).

[54] B. Braunecker and P. Simon, Phys. Rev. Lett. **111**, 147202 (2013).

[55] J. Klinovaja, P. Stano, A. Yazdani, and D. Loss, Phys. Rev. Lett. **111**, 186805 (2013).

[56] R. Pawlak, M. Kisiel, J. Klinovaja, T. Meier, S. Kawai, T. Glatzel, D. Loss, and E. Meyer, npj Quantum Inf. **2**, 16035 (2016).

[57] S. Das Sarma, Nat. Phys. **19**, 165 (2023).

[58] J. Wiersig, Phys. Rev. Lett. **112**, 203901 (2014).

[59] H. Hodaei, A. U. Hassan, S. Wittek, H. Garcia-Gracia, R. El-Ganainy, D. N. Christodoulides, and M. Khajavikhan, Nature (London) **548**, 187 (2017).

[60] W. Chen, Ş. Kaya Özdemir, G. Zhao, J. Wiersig, and L. Yang, Nature (London) **548**, 192 (2017).

[61] J. L. Miller, Phys. Today **70**, 23 (2017).

[62] J. Wiersig, Photon. Res. **8**, 1457 (2020).

[63] M. V. Berry, Czech. J. Phys. **54**, 1039 (2004).

[64] N. Moiseyev, *Non-Hermitian Quantum Mechanics* (Cambridge University Press, Cambridge, 2011).

[65] W. Heiss, J. Phys. A: Math. Theor. **45**, 444016 (2012).

[66] T. Kato, *Perturbation Theory for Linear Operators*, Vol. 132 (Springer Science & Business Media, Berlin, 2013).

[67] A. Ghatak and T. Das, J. Phys.: Condens. Matter **31**, 263001 (2019).

[68] H. Xu, D. Mason, L. Jiang, and J. Harris, Nature (London) **537**, 80 (2016).

[69] P. San-Jose, J. Cayao, E. Prada, and R. Aguado, Sci. Rep. **6**, 21427 (2016).

[70] S. Wang, B. Hou, W. Lu, Y. Chen, Z. Zhang, and C. Chan, Nat. Commun. **10**, 832 (2019).

[71] M.-A. Miri and A. Alù, Science **363**, eaar7709 (2019).

[72] T. Yoshida, R. Peters, N. Kawakami, and Y. Hatsugai, Phys. Rev. B **99**, 121101 (2019).

[73] N. Okuma and M. Sato, Phys. Rev. Lett. **123**, 097701 (2019).

[74] R. Okugawa and T. Yokoyama, Phys. Rev. B **99**, 041202(R) (2019).

[75] J. C. Budich, J. Carlström, F. K. Kunst, and E. J. Bergholtz, Phys. Rev. B **99**, 041406(R) (2019).

[76] T. Yoshida and Y. Hatsugai, Phys. Rev. B **100**, 054109 (2019).

[77] K. Kawabata, T. Bessho, and M. Sato, Phys. Rev. Lett. **123**, 066405 (2019).

[78] Z. Yang, A. P. Schnyder, J. Hu, and C.-K. Chiu, Phys. Rev. Lett. **126**, 086401 (2021).

[79] L. Li, C. H. Lee, and J. Gong, Phys. Rev. Lett. **124**, 250402 (2020).

[80] M. M. Denner, A. Skurativska, F. Schindler, M. H. Fischer, R. Thomale, T. Bzdušek, and T. Neupert, Nat. Commun. **12**, 5681 (2021).

[81] E. J. Bergholtz, J. C. Budich, and F. K. Kunst, Rev. Mod. Phys. **93**, 015005 (2021).

[82] I. Mandal and E. J. Bergholtz, Phys. Rev. Lett. **127**, 186601 (2021).

[83] M. Stålhammar and E. J. Bergholtz, Phys. Rev. B **104**, L201104 (2021).

[84] R. Aquino and D. G. Barci, Phys. Rev. B **102**, 201110(R) (2020).

[85] J. A. S. Lourenço, G. Higgins, C. Zhang, M. Hennrich, and T. Macrì, Phys. Rev. A **106**, 023309 (2022).

[86] Y. Para, G. Palumbo, and T. Macri, Phys. Rev. B **103**, 155417 (2021).

[87] J. Cayao and A. M. Black-Schaffer, Phys. Rev. B **105**, 094502 (2022).

[88] R. Schäfer, J. C. Budich, and D. J. Luitz, Phys. Rev. Res. **4**, 033181 (2022).

[89] Y. Ashida, Z. Gong, and M. Ueda, Adv. Phys. **69**, 249 (2020).

[90] P. Delplace, T. Yoshida, and Y. Hatsugai, Phys. Rev. Lett. **127**, 186602 (2021).

[91] N. Hatano and D. R. Nelson, Phys. Rev. Lett. **77**, 570 (1996).

[92] Z. Gong, Y. Ashida, K. Kawabata, K. Takasan, S. Higashikawa, and M. Ueda, Phys. Rev. X **8**, 031079 (2018).

[93] K. Kawabata, K. Shiozaki, M. Ueda, and M. Sato, Phys. Rev. X **9**, 041015 (2019).

[94] M. Ezawa, Phys. Rev. B **98**, 201402(R) (2018).

[95] See Supplemental Material at http://link.aps.org/supplemental/10.1103/PhysRevB.108.L060506 for we discuss how the results present in the main text change with different parameters. In particular, we show finite-size effects, the effect of a finite chemical potential, and the absence of the enhancement for periodic boundary conditions. Further, we establish analytically the exceptional enhancement shown in the main text, and we revise the literature on the non-Bloch formalism and Green's function approach to non-Hermitian

systems. The Supplemental Material includes videos, which illustrate how the properties described in the main text evolve for a continuous change of parameters. The color bars used there have the same scale as the one used in the main text and in the Supplemental Material.

[96] L. L. Sánchez-Soto, J. J. Monzón, A. G. Barriuso, and J. F. Cariñena, Phys. Rep. **513**, 191 (2012).

[97] Y. Fu and S. Wan, Phys. Rev. B **105**, 075420 (2022).

[98] H. Li and S. Wan, Phys. Rev. B **105**, 045122 (2022).

[99] J. Feinberg and A. Zee, Nucl. Phys. B **504**, 579 (1997).

[100] P. O. Sukhachov and A. V. Balatsky, Phys. Rev. Res. **2**, 013325 (2020).

[101] S. Datta, *Electronic Transport in Mesoscopic Systems* (Cambridge University Press, Cambridge, 1997).

[102] S. Yao and Z. Wang, Phys. Rev. Lett. **121**, 086803 (2018).

[103] C. H. Lee and R. Thomale, Phys. Rev. B **99**, 201103(R) (2019).

[104] C. H. Lee, L. Li, R. Thomale, and J. Gong, Phys. Rev. B **102**, 085151 (2020).

[105] P.-G. De Gennes and P. A. Pincus, *Superconductivity of Metals and Alloys* (CRC Press, Boca Raton, 2018).

[106] J.-X. Zhu, *Bogoliubov-de Gennes Method and Its Applications*, Vol. 924 (Springer, Berlin, 2016).

[107] F. K. Kunst and V. Dwivedi, Phys. Rev. B **99**, 245116 (2019).

[108] V. M. Martinez Alvarez, J. E. Barrios Vargas, and L. E. F. Foa Torres, Phys. Rev. B **97**, 121401(R) (2018).

[109] S. Longhi, Phys. Rev. Lett. **124**, 066602 (2020).

[110] S. Longhi, Phys. Rev. Res. **1**, 023013 (2019).

[111] B. Gardas, S. Deffner, and A. Saxena, Sci. Rep. **6**, 23408 (2016).

[112] J. Wiersig, Phys. Rev. Res. **4**, 023121 (2022).

[113] Y. Cao, V. Fatemi, A. Demir, S. Fang, S. L. Tomarken, J. Y. Luo, J. D. Sanchez-Yamagishi, K. Watanabe, T. Taniguchi, E. Kaxiras, R. C. Ashoori, and P. Jarillo-Herrero, Nature (London) **556**, 80 (2018).

[114] Y. Cao, V. Fatemi, S. Fang, K. Watanabe, T. Taniguchi, E. Kaxiras, and P. Jarillo-Herrero, Nature (London) **556**, 43 (2018).

[115] L. Balents, C. R. Dean, D. K. Efetov, and A. F. Young, Nat. Phys. **16**, 725 (2020).

[116] E. Y. Andrei and A. H. MacDonald, Nat. Mater. **19**, 1265 (2020).

[117] H. Zhou, T. Xie, T. Taniguchi, K. Watanabe, and A. F. Young, Nature (London) **598**, 434 (2021).

[118] H. Zhou, L. Holleis, Y. Saito, L. Cohen, W. Huynh, C. L. Patterson, F. Yang, T. Taniguchi, K. Watanabe, and A. F. Young, Science **375**, 774 (2022).

[119] E. C. Marino, *Quantum Field Theory Approach To Condensed Matter Phys.* (Cambridge University Press, Cambridge, 2017).

[120] V. Kozii and L. Fu, arXiv:1708.05841.

[121] D. S. Borgnia, A. J. Kruchkov, and R.-J. Slager, Phys. Rev. Lett. **124**, 056802 (2020).

[122] N. Okuma, K. Kawabata, K. Shiozaki, and M. Sato, Phys. Rev. Lett. **124**, 086801 (2020).

[123] K. Zhang, Z. Yang, and C. Fang, Phys. Rev. Lett. **125**, 126402 (2020).

[124] L. Li, C. H. Lee, S. Mu, and J. Gong, Nat. Commun. **11**, 5491 (2020).

[125] T. Helbig, T. Hofmann, S. Imhof, M. Abdelghany, T. Kiessling, L. Molenkamp, C. Lee, A. Szameit, M. Greiter, and R. Thomale, Nat. Phys. **16**, 747 (2020).

[126] L. Xiao, T. Deng, K. Wang, G. Zhu, Z. Wang, W. Yi, and P. Xue, Nat. Phys. **16**, 761 (2020).

[127] F. K. Kunst, E. Edvardsson, J. C. Budich, and E. J. Bergholtz, Phys. Rev. Lett. **121**, 026808 (2018).

[128] K. Yokomizo and S. Murakami, Phys. Rev. Lett. **123**, 066404 (2019).

[129] X. Zhang, G. Li, Y. Liu, T. Tai, R. Thomale, and C. H. Lee, Commun. Phys. **4**, 47 (2021).

[130] F. Song, S. Yao, and Z. Wang, Phys. Rev. Lett. **123**, 170401 (2019).

[131] Z. Yang, K. Zhang, C. Fang, and J. Hu, Phys. Rev. Lett. **125**, 226402 (2020).

[132] T. Yoshida, T. Mizoguchi, and Y. Hatsugai, Phys. Rev. Res. **2**, 022062(R) (2020).

[133] S. Diehl, E. Rico, M. A. Baranov, and P. Zoller, Nat. Phys. **7**, 971 (2011).

[134] E. C. Stoner, Proc. R. Soc. London A **165**, 372 (1938).

[135] J.-P. Pouget, C. R. Phys. **17**, 332 (2016).

[136] S. Sayyad and F. K. Kunst, Phys. Rev. Res. **4**, 023130 (2022).

[137] R. Arouca, E. Marino, and C. M. Smith, Quantum Front. **1**, 2 (2022).